SLAMMING QUASI-STATIC ANALYSIS OF AN INCAT 98-m HIGH-SPEED WAVE PIERCING CATAMARAN.

W. Amin, School of Engineering, University of Tasmania, Hobart, Australia, **M. R. Davis**, School of Engineering, University of Tasmania, Hobart, Australia, **G. A. Thomas**, Australian Maritime College, University of Tasmania, Launceston, Australia, and **D. S. Holloway,** School of Engineering, University of Tasmania, Hobart, Australia.

SUMMARY

A "Reverse Engineering" approach to investigate slamming loads on large high-speed wave piercers is used in conjunction with trials data and finite element analysis. Trials data are used to develop the loading conditions during severe slamming events in terms of the vessel motions and immersion. The underlying wave loads are applied to a global FE model, in addition to a complementary slamming load. The longitudinal and transverse slam load distribution was based on pressure measurements during model tests. The load location and magnitude were then systematically changed until the best match between trials and FE strains was achieved. The results show that the comparison method with trials is critical and suggests that FE dynamic analysis is required to fully understand and develop realistic interpretation of slamming loads during trials.

NOMENCLATURE

$BVACC$	Bow vertical acceleration (g)
$GVACC$	Ship's CG vertical acceleration (g)
$RBVV$	Relative bow vertical velocity (m/s)
RBH	Relative bow height (m)
cc	Correlation coefficient
n	size of data sample set
MSE	Mean square error
$RMSE$	Root mean square error
$NRMSE$	Normalised RMSE
I_s	Impulse on ship (Ns, tonne s)
I_m	Impulse on model
F_s	Slam Load (N, tonne)
M_s	Moment due to F_s (Nm, tonne m)
x_s	F_s location WRT a strain gauge location (m)
E	modulus of elasticity (N/m^2)
Z	Section modulus at strain gauge location (m^3)
t_1	Slam start instant (s)
t_2	Slam end instant (s)
V_m	Model speed (m/s)
V_s	Ship speed (m/s)
L_s	Ship length (m)
L_m	Model length (m)
SE_F	FE total strain energy (J, tonne m)
SE_{cf}	Strain energy calibration factor
ε_F	Finite element strain
ε_T	Trials strain
σ_F	Standard deviation of FE strains
σ_T	Standard deviation of trial strains

1. INTRODUCTION

The demand for high speed sea transportation has increased rapidly in the last three decades, addressing new operational problems regarding ship motions and hull strength. Structural response due to slamming becomes a major concern during high speed and rough sea operations, especially for those ships approaching 100 m in length. The advanced hull configuration of wave piercers has introduced new aspects and scenarios of slamming that has never existed in conventional ships. The introduction of a centre bow that characterises this kind of high-speed ships confers obvious improvements of seaworthiness and safety of catamarans especially in following seas as well as to reduce extreme pitching motion. However, high flare forward of the jaws area (where the upper edge of the demi-hull meets the lower edge of the centre bow) and the enclosed space between the centre bow and the demi-hulls, known as an arch, can causes high impact loads which are different from those experienced on other conventional ships such as bottom and bow slamming. Severe slamming events may result in global damage such as side shell buckling and bow damage, and/or local structural damage such as dishing of plating, stiffener tripping, buckling and cracking.

The vessel under consideration in this study is Hull 061, built by INCAT Tasmania, and designed by Revolution Designs Pty Ltd, which is originally a high-speed passenger ferry but subsequently configured to US Navy specification for military purposes and is known as HSV-2 SWIFT. The ship underwent an extensive trials program to investigate the applicability of using this advanced hull form in severe sea operations as well as determining her operational envelope. The importance of these trials, with regard to slamming, is that the ship did not change course nor her velocity in response to severe slams unlike other trials for commercial vessels where ship masters tend to reduce speed if severe slamming is sustained. However, response alarms were set up previously based on

Revolution Design recommendations and were rarely reached during the trials. Trials of 061 were conducted by Naval Surface Warfare Centre, Carderock Division, US Navy and resulted in 211 runs at different sea conditions, speeds and headings. Full details of trials, the data acquisition system and instrumentation can be found in [1] and [2]. High values of vertical accelerations up to 1.21 g at LCG and 5.41g at bow were reported, [3]. The available runs for full analysis were Hat1_59 for head sea conditions. It was noted that all the gauges had an inconsistent bias; this bias was removed so that a mean value of zero is set up for all gauges, which means that at the still water condition before departure all signals from all gauges should be zero. The same procedure was applied for the motion data; bias was removed from all accelerations (at the bow and centre of gravity) and roll angle. The situation for pitch angle and relative bow motion was different. The ship had a static trim at departure of about 1 m by the bow, [4]. At this condition, the trim angle was 0.702 degrees and therefore, the mean of the pitch angle during trials should have this value based on the assumption that the change in LCG due to fuel consumption and other consumables is minimal. The validity of this assumption held due to the close position of the trial course from the departure point (about 50 nautical miles), [2]. The same procedure was applied to the relative bow motion record. The distance between the sensor location and the still water height was calculated based on the departure condition and the drawings supplied by INCAT for the sensor location details. The calculations led to a static bow height of 6.45m, which should be the mean of the relative bow height signal. The wave height signal was de-biased so that it has a zero mean.

The longitudinal bending response was monitored by six strain gauges located on the demi-hull keel centre girders port and starboard, about 30 cm forward of the reference frame and approximately mid-height of the centre girder. The keel gauges will be referred to as T1_5, 6 and 7 on the port side and T1_8, 9 and 10 on the starboard side at Fr 25, 46 and 61 respectively (frame spacing is 1.2 m, Fr 0 at the transom). The vertical steel posts, port and starboard, Fr 62, were equipped with strain gauges to investigate their response to global slamming loads and were positioned 50 cm away from the connection to the mission deck. They will be referred to as T_2 and T2_3 for port and starboard location respectively.

2. SCOPE OF WORK

The principal motivation behind the exploration of slamming load by means of FE analysis and "Reverse Engineering" procedures is the low reliability of the available predictive codes to estimate the whipping response due to impact loads. The suggested procedure will also provide solid grounds for the assessment and development of such codes. Therefore, a "Reverse Engineering" procedure using FE capabilities will advance understanding of severe slamming events in terms of load severity and location, as well as its spatial and temporal distributions. A first step towards the ultimate goal is a FE quasi-static analysis in which the slamming load is assumed to act statically, and then FE dynamic analysis in which load development time history can be input to the FE model. In this paper, the quasi-static analysis work is reported. Slamming load development and the subsequent whipping are not relevant to the current study. Slamming loads will be superimposed on an underlying wave response during the instant of the maximum slam response. The FE strains are then compared to trials strains. Based on the comparison of results the slamming load parameters will be changed systematically until a best match with trials can be achieved.

3. SIMULATION OF SLAMMING LOADS

The applicability of FE analysis as a tool to predict sea loads based on "Reverse Engineering" procedures has been discussed and tested in [5] as well as quasi-static analysis procedures for normal operating conditions without slamming. In contrast to similar studies, where calibration factors between the applied loads and strains are extracted from a hypothetical loading condition applied to the FE model, [6], [7] and [8], sea trials data, namely wave height, bow and CG vertical accelerations, pitch and relative bow height records, can be used to develop a quasi-static load case for input to the FE model. The numerical strains and trials strains are then compared. Slamming loads are usually dealt with in the same manner, i.e., calibration factors are used to convert trials strains to an "equivalent-hypothetical" static wave loading model except for the work done in [9] in which a complementary slam load with approximate wave loading condition, based on trials measurement for wave length and height, was used. The calibration factors methodology, based only on the equivalent static wave approach, in treating slamming loads does not provide any information about slamming location nor spatial distribution which is of great importance for local analysis. As an alternative, the procedure discussed in [5] will be applied in which the quasi-static sinusoidal wave loads are not exaggerated to produce the large slam response. Instead, the impact loads are dealt with as "add-on" complementary loads which will be changed systematically until a best match between FE strains and trials strains is achieved. Therefore, the loading model to be fed as input to the FE model should contain basic information about the load application area, magnitude and distribution.

The procedure can be summarised as follows:

- Define a momentary instant of slamming occurrence. At this instant, the quasi-static wave load model is developed based on sea trials data for the wave profile.
- Define an appropriate spatial distribution for the slamming load.
- Define an initial estimate for slam magnitude.

- Define an initial estimate for slam location along the boat length.
- Compare FE strains and trials strains
- Revise estimates of slam magnitude and location
- Repeat analysis until a satisfactory match is achieved.

3.1 THE INSTANT OF SLAM OCCURRENCE

An instant during the trials is required to develop the load model. This instant should be related to the slamming event development. A typical severe slamming event is shown in Figure 1.

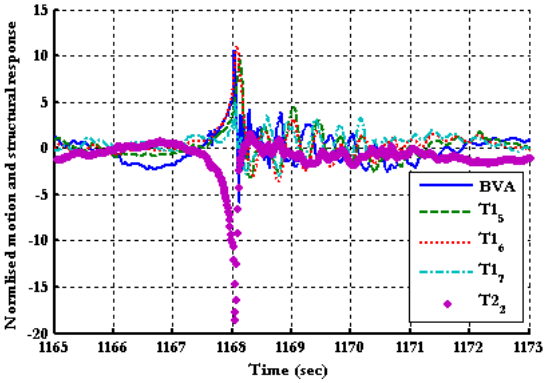

Figure 1: Typical slamming event time histories of bow vertical acceleration and strain gauge records.

The figure shows the vertical bow acceleration, the port side keel gauges and the vertical steel post gauge, each record is normalised to its standard deviation Three instants can define the temporal development of a severe slamming event, though only one of them can be defined accurately which is the maximum response instant. The first instant is the slam initiation instant, when the response starts to build up over the normal wave response. This instant cannot be defined accurately but approximately one can choose the standard deviation of the whole signal as a limit beyond which the slam is regarded to commence building-up. The second instant is in between the former instants when there is a sudden change in the rate of response values. In the current study, only the maximum response is of the interest and this is easily defined for severe events. The identification of this instant becomes harder when the slams are of a smaller intensity. Visual inspection of the largest 50 slams in the available run showed that the peak instant of the vertical bow acceleration preceded all other sensors peaks. Being the closest sensor to slam location, it was considered that this accelerometer could be used to identify the instant of slam occurrence.

3.2 SLAM LOAD SPATIAL DISTRIBUTION

Slamming can occur spatially on three areas; (a) the demi-hull keels, (b) the centre bow and (c) the arch area. The bottom slamming on the demi-hulls contribution to the severity of the slamming event is believed to be very small and can be neglected in most cases. Figure 2 shows the time histories of keel line emergence for a series of slams between the instants 560 and 600 sec. at frames 57 to 76.

It can be seen that the keel re-entry does not produce significant slam loads and for example its contribution to the slam at the instant 566 sec can be neglected without any consequences on the slamming response. For other slams in the record, after the instant 570 sec, the keel does not definitively contribute to the slam response as it is always immersed. The exact boundaries between the other two areas can not be

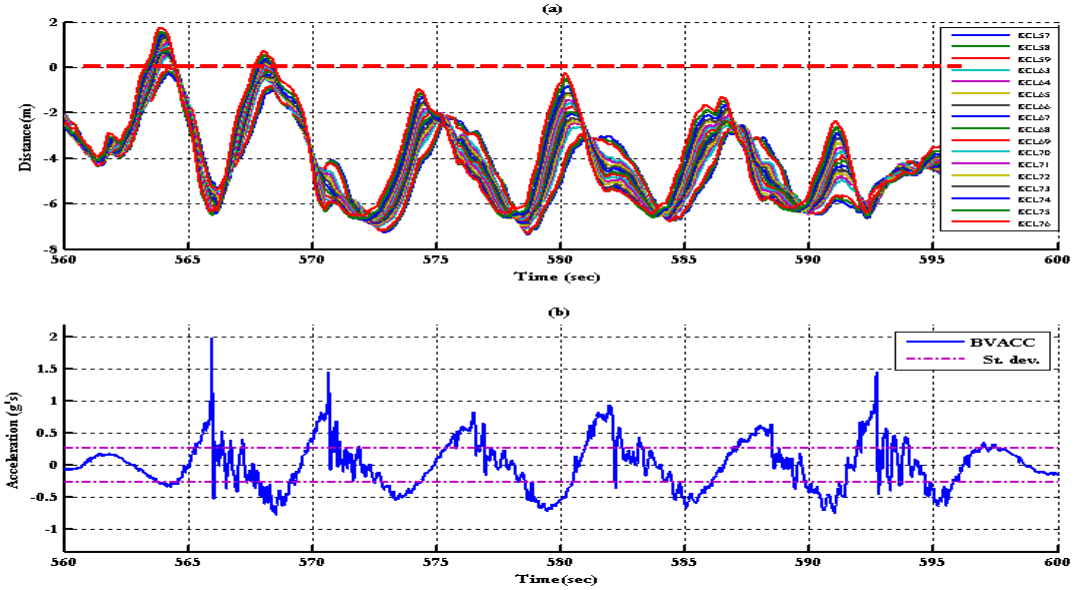

Figure 2: (a) Demi-hull keel emergence from Fr 57 to Fr 76, (b) vertical bow acceleration record.

defined due to the geometrical complexity of the bow area. However, the arch area boundaries can be defined as the area where the flare on the centre bow starts to change rapidly. Slams due to filling of the arch between the centre bow and the demi-hull were studied only during two-dimensional drop tests in calm water, [10]. The other area where slamming can occur is the rest of the centre bow, which would be similar to those slams experienced by high-speed monohulls. A similar study, [9], assumed the slam load distribution was quadratic along the arch way up to the end of the centre bow and linear in the transverse direction with its maximum midway between the centre bow and the demi-hull. Although good agreement was achieved with trials strains, the load distributions were not confirmed. To confirm the slam load distribution, model experiment pressure measurements were conducted on Hull 064, 112 m LOA. The principal dimensions of both hulls are summarised in Table 1. Pressure transducers were distributed on the wet deck and the centre bow to acquire water pressure in 84 locations. Figure 3 shows the locations of pressure transducers on the centre bow and a part of the wet deck of the segmented model of Hull 064.

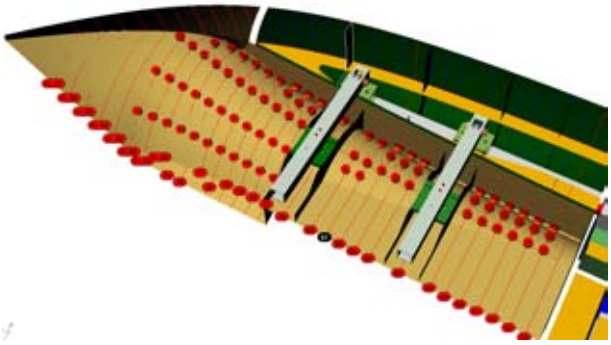

Figure 3: Transducer array for pressure measurement on the centre bow and wet deck.

	Hull 061	Hull 064
LOA (m)	98	112
LWL (m)	92.4	105.6
BOA (m)	26.6	30.5
Hull spacing (m)	21.7	24.7
Draft (m)	3.96	3.93
CB length	0.25LWL	0.19LWL
Disp.(ton.)	1845	2800
Service speed (knots)	38	40

Table 1: Hulls 061 and 064 specifications

The tests were conducted in regular wave trains. Preliminary analysis of the test results showed that the maximum pressures at each frame predominantly occur at, or very close to, the arch top. A typical longitudinal pressure distribution is shown in Figure 4. The figure shows the longitudinal pressure distribution with respect to the location of the maximum response along the arch top line. The real distribution was approximated by a linear fit, so that the impact load distribution input to the finite element model could be standardised. The transverse distribution was very similar to the distribution obtained in two dimensional drop test, [10]. The slam distribution was assumed to follow the same trend and the distribution was standardised to a second order approximation as shown in Figure 5. The distribution of the slam load to be input into the finite element model was developed based on an initial estimate of the maximum nodal slam force. Once this was assumed, the maximum nodal force at each frame could be obtained. The nodal force at each frame from the longitudinal distribution model is the maximum at this specified frame. Then, the transverse distribution could be achieved based on the assumed quadratic distribution model. According to the specified nodes of application, the nodal forces are calculated according to their locations from the top point of the arch.

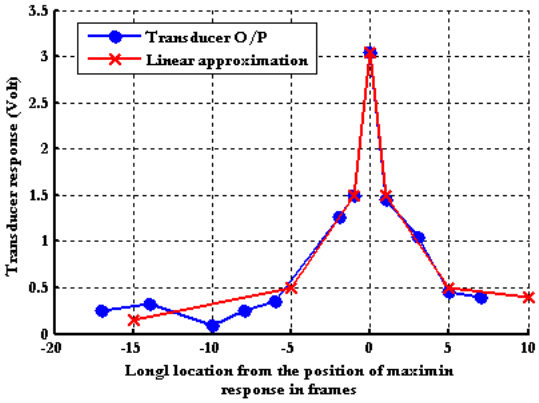

Figure 4: Proposed longitudinal pressure distribution along the top arch line.

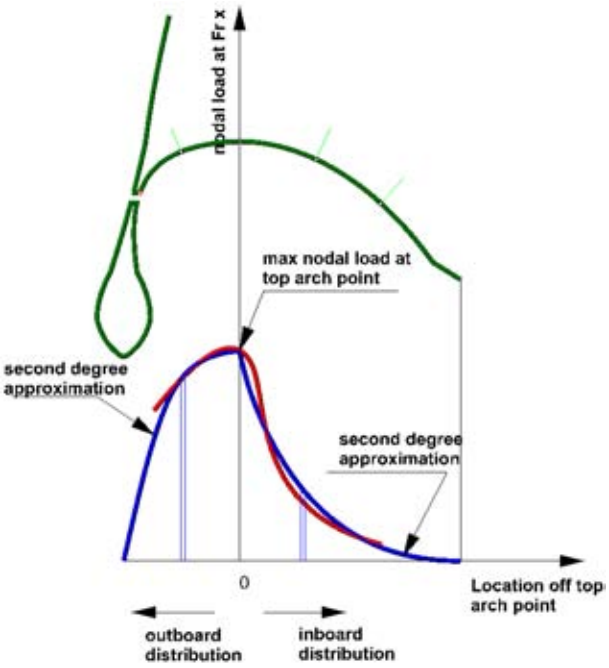

Figure 5: Proposed transverse slam distribution

4. FINITE ELEMENT MODEL

The global finite element model was prepared by Revolution Design using the software package PATRAN/NASTRAN from MSC Software. Grillages were modelled as laminates (composite layers). In this technique, the grillage components, plating, attached

stiffener webs and flanges are modelled in three layers having the same width. Plating is modelled as shell elements with stiffness in longitudinal and transverse directions (isotropic properties), stiffener webs and flanges with longitudinal stiffness only (anisotropic properties). Due to the change of the areas of web and flange layers, the material modulus elasticity for these layers is changed so that the new modulus of elasticity is equal to the original modulus of elasticity multiplied by the ratio of cross sectional areas. The main purpose for using this technique is to reduce the modelling time. However, the laminate modelling has not been assessed for its capacity to determine local strains at the locations of the strain gauges. Therefore, a fixed grillage configuration, shell plate, one transverse frame and two longitudinal stiffeners, was modelled in three different ways; (a) shell, stiffener webs and flanges as laminates, (b) plating as shell elements, stiffeners as beam elements and (c) all components modelled as shell elements. The grillage was loaded with a constant pressure load of the same value for the three models. The deformation output is shown in Figure 6.

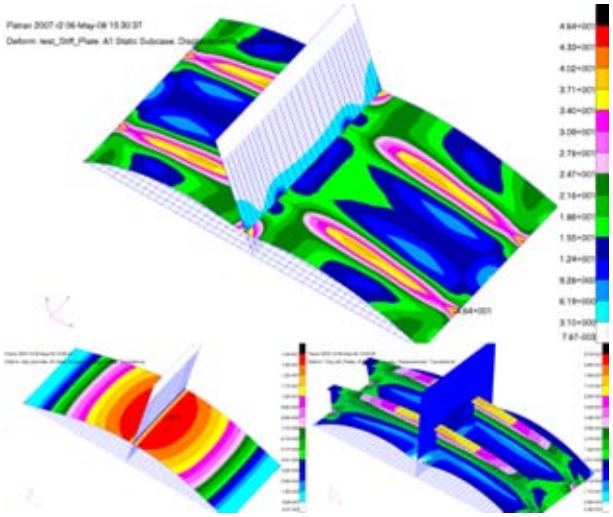

Figure 6: Deformation plots of 3 modelling technique for the same grillage structure under the same loading conditions, top: stiffeners as beam element, bottom left: laminates, bottom right: all plates.

The figure shows that the laminate modelling technique is not capable of specifying the local strain as are the other techniques. The laminate modelling succeeded in predicting the maximum strain level, but did not capture the actual strain distribution in any of the three layers. The beam elements stiffeners predicted very close strain distribution to that of all plate elements, but also represented stiffener strain only in the axial direction. The all-plate modelling technique was able to describe the strain distribution in every part of the model including the stiffener webs and flanges. Hence, it was decided to refine the strain gauge locations using the modelling technique of shell elements for plating and beam elements for stiffeners. Therefore, around the strain gauges, the keel plate, the keel centre girder and its flange and side frames were modelled as shell elements. The longitudinal stiffeners on the keel plate close to the keel centre girder were modelled as beam elements. The rest of the model was left in its original laminate modelling state. At the location of a strain gauge, a fine mesh was implemented to obtain improved strain distribution. In this work, it was decided to use a mesh around the strain gauges of 50×50 mm quadrilateral elements and to slowly increase the mesh size away from the strain gauge location as shown in Figure 7. Only the superstructure raft was modelled explicitly in the global FE model. The fully loaded superstructure mass was distributed using a combination of lumped mass elements and scaled material densities for the raft beams. The global model, after re-meshing and adjustment of weight and cargo distributions, had 91731 quad elements, 2284 triangular elements, 93123 nodes, 194 MPC elements, 77 beam sections, and 558738 DOFs.

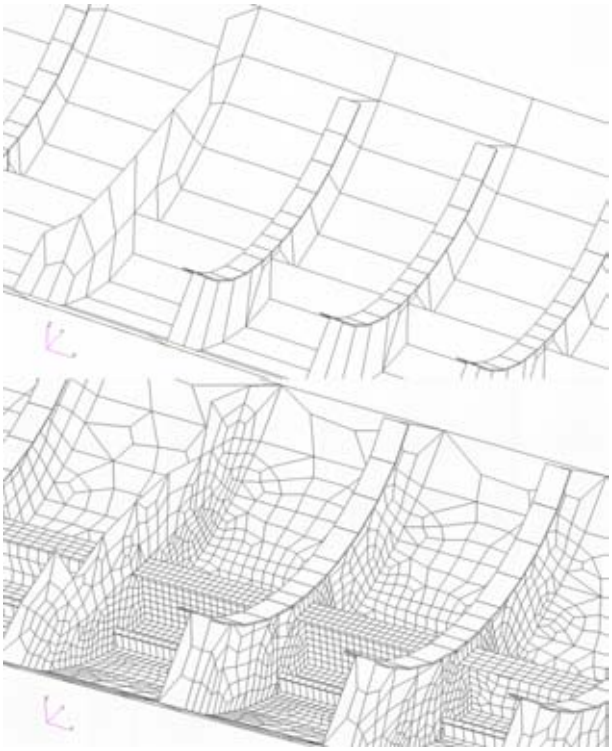

Figure 7: Original and refined mesh around the strain gauge location

Structural simplifications in the model, such as the lack of the keel centre girder flange, bracketed connections, welding details and bolted connections caused a lower lightship displacement than required and an incorrect LCG value when compared to weight sheet calculations, [11]. Much effort was conducted to achieve an LCG as close as possible to the real trials condition. An aft balance weight of 96 tonnes divided between 4 nodes located approximately 1 m aft of the transom and connected to the model by MPCs, was introduced as a correction. This is a standard technique used by Revolution Design to adjust the position of longitudinal centre of gravity and is accepted by classification society Det Norske Veritas (DNV). This

solution resulted in stress hot spots close to the transom but they are distant from the strain gauge locations under consideration and their effect is considered to be only local. The loading condition for the ship before trials was derived from the ship drafts, which were recorded before departure to be 4 m forward and 3 m aft at the draft mark locations [4]. Whilst some masses were known, such as the instrumentation trailer [1], other masses were estimated so that the required trials displacement was achieved. For Run Hat1-59, which was 50 nm distant from the departure point, the fuel load was assumed to be at full capacity, with the consumed fuel to the trial site being regarded as insignificant with respect to the ship displacement.

5. SLAM LOAD CASE DEVELOPMENT

Once the instant of slam occurrence had been identified, as discussed previously, the relative bow height, trim, vertical bow acceleration and wave height data at this instant, were extracted. The actual water profile was obtained based on the method discussed in [5], and the buoyancy forces calculated at each frame and presented as nodal loads on 3 keel nodes per frame.

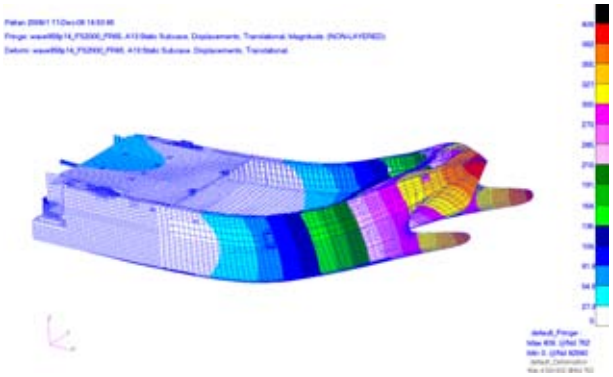

Figure 8: Exaggerated displacements plot in response to a slamming event.

The finite element load case was composed of four different loads:

(a) Gravity load which represent the vessel weight and is distributed on all nodes according to the elements material properties.

(b) The hydrostatic load due to the underlying waves, as derived from the trials based on the actual waterline.

(c) Inertia load which represents the inertia load due to the vessel acceleration at the moment of slam occurrence. The vertical motion is considered only. The longitudinal acceleration was neglected because the longitudinal forces of thrust and resistance were not present in the FE model.

(d) The slam load. The application area of the slam load was predefined in the MATLAB code as a list of nodes. The list was divided into groups according to the load distribution function. The slam load was calculated at each node and represented in the FE model as nodal loads.

An initial estimate of the maximum nodal load and its longitudinal location are input to the MATLAB code, and then a slam load case was ready to be input into the FE model for analysis. The FE solver MSC NASTRAN uses the technique of inertia relief to counter balance any non-equilibrium in the applied forces. In the output file, the inertia relief applied forces should be checked When these forces are small, it means that the applied loads are in good balance. An exaggerated displacement response to a slamming event from the FE analysis is shown in Figure 8

6. COMPARISON WITH TRIALS

The comparison with the trials is very critical to this type of analysis. Generally, in the case of quasi-static analysis, two approaches exist. One approach is to compare the FE results to the maximum response of each strain gauge during the slam event. The second is to compare the FE results to the instantaneous trials strains only at the moment of slam occurrence. Both approaches were investigated. Three slams were studied with maximum peak accelerations at the instants 710.89 s, 773.89 s and 856.14 s. The slamming particulars at these instants are shown in Table 2. A total number of 42 load cases were established and run for both approaches for the three slams. As an example, FE strains and trials strains are plotted in Figure 9 for the severest slam in the record under consideration at the instant 856.14 s. The suffix s in the figure's legend denotes the simultaneous strain comparison approach while no suffix denotes the peak strain comparison approach. It should be noted that the derived FE strains were corrected first before comparison with trials by subtracting the still water response from values obtained during slam simulation. This correction was verified when dealing with normal wave loading only as discussed in [5]. The figure shows that the simultaneous trials strains were significantly lower than trials peaks of all strains during the slamming event by about 40% towards the stern and amidships and 30% forward. This was due to the nature of the impact that occurs in the forward part of the ship and the propagation of the transient loading wave though the structure, which results in strain peaks time delayed from the instant of the maximum vertical bow acceleration.

Slam Event	856.14s	710.89s	773.89s
Max BVACC (g)during event	3.03	2.24	1.72
Max. GVACC(g)during event	0.76	0.39	0.36
Max.RBVV(m/s) before event	5.13	4.4	4.05
WH (m) during event	6.81	2.24	2.02
Min RBH (m) during event	0.11	2.98	3.61
Max pitch before event	5.01	3.36	2.89

Table 2: Particulars of slamming events under consideration.

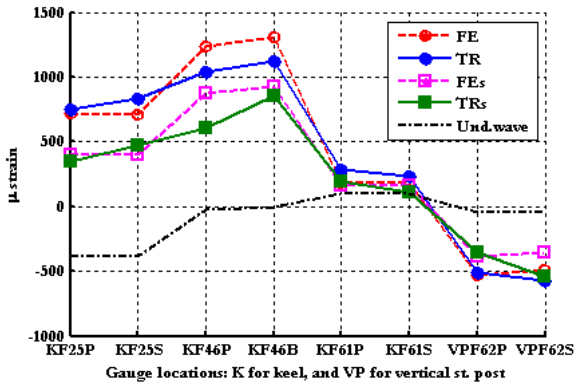

Figure 9: Comparison between FE strains and trials for slam at 856.14 sec.

Figure 9 also shows the underlying wave response of each gauge. It can be noted that the structural strain is at a minimum in the forward half of the ship and increases considerably towards the stern to a level that is equal to the simultaneous trials strains but opposite in direction. The location of the slam load was predicted to have its maximum at Fr 65 for both cases with the resultant slam load nearly at Fr 64, 8 frames forward of the aft end of the centre bow. This location is nearly 83% of LWL from the transom. In experimental studies on Hull 064 model, the slam load resultant was measured to be approximately one frame (1.2m) forward of the centre bow aft end. This corresponds to about 81% of LWL. It should be noted that the centre bow extension in Hull 061 (25% LWL) was longer than Hull 064 (19%LWL).

Table 3 summarises the predicted total slam load for each of the three slams and the applied comparison approaches. The table shows that the severest slam load reached a value of 3137 tonnes (1.7 times the ship displacement) when the FE strains were compared to peak strains of all gauges during the slamming event. This value was reduced to 2241 tonnes (1.21 times the ship displacement) with a difference of 48%. The same occurred for the other two slams but with a reduction in the difference between the two approaches down to 14%.

Comparison approach	(a) Peak trials strains approach.			(b) Simultaneous. Trials strain approach.		
	856.14s	710.89s	773.89s	856.14s	710.89s	773.89s
Load (tonne)	3137	1891	837	2241	1543	578
Loc. (%LWL)	83.1	75.3	79.2	83.1	74	81.8
Load/Disp	1.7	1.025	0.454	1.215	0.836	0.313
Correl. %	97.2	96.4	93	97.1	94	82
NRMSE	6.8	11.7	14.7	8.9	11.2	23.5

Table 3: Comparison of FE and trials strains based on (a) peak trials strain and (b) simultaneous trials strains.

The table also shows that the resultant slam load location for these slams is between 74% and 83.1 % LWL from the transom. Experimental work on the Hull 064 model showed that the resultant slam load is mostly located around the aft end of the centre bow which corresponds to about 78% to 80% LWL from the transom. The centre bow of Hull 064 is 19% LWL long. The extended length of the centre bow on Hull 061, 25% LWL might be the reason of the longer range of slam locations on Hull 061 which was expected where the water is likely to be trapped between the centre bow and the demi-hulls.

A similar study for Hull 050 (LOA 96 m), [12], concluded a slamming load of about 1280 tons which is nearly half of the current slam load based on a simultaneous strain analysis. The reason behind this differebnce in largest observed slam loads might be the severe trials conditions for Hull 061where the vessel speed was 20 knots at sea state 5 while Hull 050 experienced the slam mentioned at speed of 15 knots at sea state 4 and 140° heading (starboard bow at 40°).

Two measures were used for evaluating the comparison between trials strains and computed strains, the correlation coefficient which is defined by:

$$cc(\varepsilon_T, \varepsilon_F) = \frac{\sum_{i=1}^{n}[(\varepsilon_{F_i} - \bar{\varepsilon}_F)\cdot(\varepsilon_{T_i} - \bar{\varepsilon}_T)]}{n \cdot \sigma_F \cdot \sigma_T} \qquad (1)$$

and an error function based on the mean square error; MSE and the data range, MSE is defined as:

$$MSE = \frac{\sum_{i=1}^{n}(\varepsilon_{F_i} - \varepsilon_{T_i})^2}{n} \qquad (2)$$

The MSE has the squared units of the data and it was more convenient to express the average error as the RMSE, which is the square root of the mean-squared-error. The RMSE value can be used to compare several possible fits. The best fit is the one with the lowest RMSE. For the current application, it is more meaningful if the RMSE is normalised by the range or the standard deviation of the trials data.

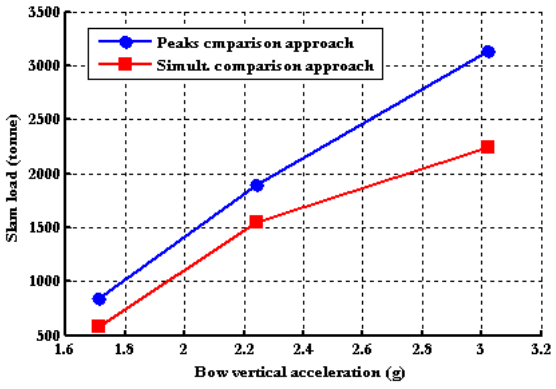

Figure 10: Slam load estimation according to the comparison approach with trials strains

Dividing by the data range could be misleading when the sample contains spikes, which are not throughout the sample, which is not the current case. Therefore, it was decided to represent the RMSE as a percentage of the trials strain range; namely the normalised root-mean-square-error NRMSE, Table 3. The difference in predicted slam loads according to the two comparison approaches is shown in Figure 10. For the most severe

slam experienced in head seas, a difference of 45% is found between the two approaches. This difference is reduced to 14% for the weakest slam under consideration

7. THE QUASI-STATIC IMPULSE

A typical slamming event is shown in Figure 11. The figure shows the vertical bow acceleration time record and the whole signal standard deviation.

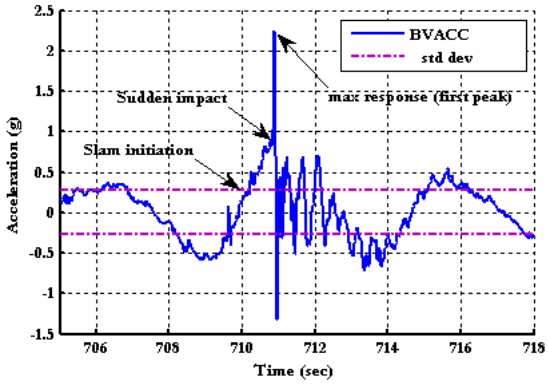

Figure 11: Typical slamming event showing the instants of concern and the record standard deviation

Two distinct instants of interest to slam duration are defined; the slam initiation instant at which the slam starts to evolve gradually and the impact instant when a sudden change of the response gradient is noticeable. The first instant can be chosen as the instant when the load exceeds the normal underlying wave loads. However, this is hard to define. Instead, this instant was chosen when the response was equal to the standard deviation of the whole signal. Either of the two instants can be taken as the slam start time. In the following analysis, the former is chosen because it describes the impulse as a superposition on the underlying wave load.. It is believed that the sudden impact corresponds to the slamming force at the arch top. However, this does not preclude slam occurrence on the centre bow itself at lower surface elevations. Similarly, the impact end instant is not known and in this case the end instant was assumed to coincide with the intersection of the standard deviation line on the right hand side of the maximum response. By assuming that the slam force can be dealt with as a resultant F_s acting at a distance x from the strain gauge under consideration, and neglecting the underlying wave loads including the added mass, the inertia forces and gravity forces, then the impulse due to slam I_s can be defined as:

$$I_s = \int_{t1}^{t2} F_s dt \cong \int_{t1}^{t2} \frac{M_s}{x_s} dt = \int_{t1}^{t2} \frac{\varepsilon_T EZ}{x_s} dt = \frac{EZ}{x_s} \int_{t1}^{t2} \varepsilon_T dt \qquad (3)$$

The section modulus was derived from the finite element model using the section tool in PATRAN. The lower and upper integration limits were taken as discussed above. Table 4 shows a summary calculation for the three slamming events based on the aft keel gauge; T1_5, Fr 25 as an example. The slam force location is the position of the resultant force measured from the transom. The strain integration is multiplied by 10^{-6} as its units are in micro strain. The integral was evaluated numerically using the trapezoidal rule at 0.01 sec intervals.

Slam Inst.	710.89s	773.89s	856.14s
t_1	710.21	773.2	855.68
t_2	711.15	774.12	856.44
Fs	1543	578	2241
Location (m)	68.64	75.84	77.04
x (m)	12.84	20.04	21.24
$\int_{t_1}^{t_2} \varepsilon dt$	1.44e-04	1.25e-04	2.15e-04
I_s (tonne.sec)	51.437	37.689	62.965

Table 4: Quasi-static impulse prediction based on keel gauge T1_5, Fr 25, for three slamming events.

It was found that the forward gauges produce higher impulses than the aft gauges which was expected due to energy losses of the structural deformation wave when it propagates through the structure. The maximum impulses, as seen from the forward keel gauges, reached 286 tonne sec for the severest slam at the instant 856.14 s. This returns a slam duration of 0.127 sec. The model tests on Hull 064 showing comparable impulse values when scaled to full scale. For a non-dimensional encounter frequency, ω_e^*, around 3.8, which is very close to the conditions of the slam at the instant 856.14 and at a speed of 1.53 m/sec (corresponding to 20 knots ship speed), the model experienced an impulse of 5 N sec. This impulse when scaled to the full ship according to the relation:

$$I_s = I_m \frac{V_s}{V_m} \left(\frac{L_s}{L_m} \right)^3 \qquad (4),$$

returned a full scale impulse of 305 tonne sec. The current analysis for Hull 061 returned an impulse of 286 tonne sec, which is reasonable considering the smaller hull size of 061.

The energy imparted to the structure can be obtained from the FE analysis. Figure 12 shows data on the total strain energy of the FE model due to the applied loads (the four load combination mentioned earlier). The individual gauge response contributions to the total strain energy can be related through a contribution factor that is estimated as:

$$SE_{cf} = \frac{SE_F}{\varepsilon_F^2} \quad (5)$$

Therefore, an approximate prediction to the total energy imparted to the structure during a slamming event can be obtained by multiplying these contribution factors by the actual trial strains and averaging over all gauges. The strain energies estimated from the keel gauges for the three slams are plotted against the slam load as shown in Figure 12.

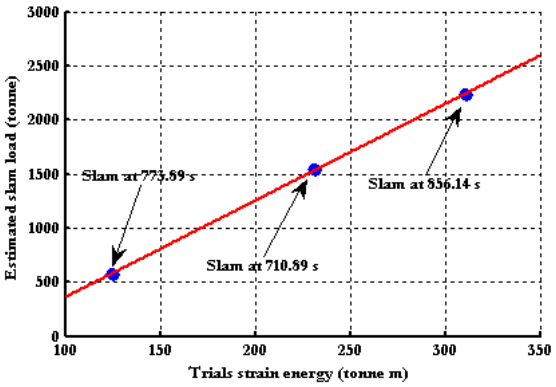

Figure 12: Estimated slam load (based on simultaneous strain analysis) versus trials strain energy

The figure shows that the relationship is almost linear which indicates that the strain energy due to underlying wave loads is negligible when compared to the slam load energy input.

8. CONCLUSIONS

A "reverse engineering" procedure, employing FEA capabilities and sea trials data, can be used in quasi-static analysis of slam loads. Confidence in the results obtained arose from realistic load distributions which are based on pressure measurements during model tests. Although the model tests were carried out in regular waves, they gave good guidance in applying the slam loads properly during numerical simulations in rough seas. However, the comparison with trials has led to a choice concerning the basis of comparison of trial strains to FE strains. Two approaches were suggested. The first is to consider the peak trials strains during the event irrespective of their time deviations from the instant of slam occurrence. The second is to consider the simultaneous strain values at the instant of slam occurrence irrespective of the maximum strain response during the event. The results show an increase of calculated slam load by 45% in the severest event when using the peak values. This difference decreases for smaller slams down to 14%.

An approximate method is proposed to evaluate the impulse and the impulsive force effective duration. FEA showed that the energy imparted to the structure can be up to 310 tonne m and an impulse of 286 tonne sec based on the forward keel gauges. It was also noted that the impulse decreases to about one fifth of the impulse at the forward keel gauges, when aft gauges are considered

The difference in results according to the approache adopted suggests that quasi-static analysis in general is not the best approach to study slamming responses as it does not take into consideration the evolving nature of slamming events and the effect of transient loading wave propagation through the structure. This results in time delays in gauge responses from the moment of slamming occurrence. Future work will use FE dynamic analysis methods to develop a more complete analysis of the slamming mechanism. Notwithstanding the magnitudes of the slam loads reported during the severe sea trials on INCAT hull 061, it is noteworthy that the vessel has suffered no structural damage during these trials.

9. ACKNOWLEDGMENT

The authors would like to thank Mr Gary Davidson and Mr Tim Roberts of Revolution Design for their valuable input into this work. In particular Mr Davidson's advice concerning finite element modelling is acknowledged.

10. REFERENCES

[1] T. F. Brady, B. R.J., M. J. Donnelly, and D. B. Griggs, "HSV-2 Swift Instrumentation and Technical Trials Plan," Naval Surface Warfare Center, Cardrock Division, Report NO: NSWCCD-65-TR-2004/18, 2004.

[2] R. J. Bachman, D. A. Woolaver, and M. D. Powell, "HSV-2 Swift Seakeeping Trials," Naval Surface Warfare Center, Cardrock Division, USNavy, Report NO: NSWCCD-50-TR-2004/052, 2004.

[3] T. Applebee, "Data Summary of Higest Five Vertical Bow Accelerations for HSV-2Swift Octagons during Feburary and May 2004," Naval Surface Warfare Center, Cardrock Division, Report NO: 5500/0421, 2004.

[4] T. F. Brady, "Swift (HSV-2) Blue Games Structural Response Summary, Quicklook Report," Naval Surface Warfare Cwnter, Cardrock Division, Report NO: NSWCCD-65-TR-2004, 2004.

[5] W. Amin, M. R. Davis, and G. Thomas, "Evaluation of finite Element Analysis as a Tool to Predict Sea Loads with the Aid of Sea Trials Data," proceedings of High Speed Marine Vehicles, Naples, Italy, pp. 1-12,2008

[6] J. Sikora, H. Paul, and S. Brian, "DTRC report," DTRC, Report NO: SSPD-91-173-43, 1991.

[7] B. Hay and J. Bourne, "Characteristics of Hydrodynamic Loads Data for a Naval Combatant," proceedings of International Conference on

Hydroelasticity in Marine Technology, pp. 169-187,1994

[8] J. P. Sikora, H. M. Ford, and J. L. Rodd, "Seaway Induced Loads and Sructural Response of the HSV-2," Naval Surface Warfare Center, Cardrock Division, Report NO: NSWCCD-65-TR-2004/11, 2004.

[9] G. Thomas, "Wave Slam Response of Large High Speed Catamarans",PhD Thesis, in Department of Mechanical and Civil Engineering, University of Tasmania, 2003.

[10] J. R. Whelan, "Wetdeck Slamming of Catamarans with Centre Bow",PhD Thesis, in Civil and Mechanical Engineering, Tasmania, 2004.

[11] Revolution Design, "MSC 061 Summary Weight Estimate," Report NO: MSC 061-99-30-005, 2003.

[12] G. Thomas, M.R.Davis, D. Holloway, and T. roberts, "Extreme Asymmetric Slam Loads on Large High Speed Catamarans," proceedings of High Speed Marine Vehicles, Naples, Italy,2002

11. AUTHORS BIOGRAPHY

Walid Amin holds a BSc (1995) and MSc (2000) in Naval Architecture and Marine Engineering at Alexandria University, Egypt. Mr Amin works as an Assistant Lecturer at the same department and is currently a PhD candidate at University of Tasmania. He has also worked in consultancy as a naval architect and design engineer in the field of offshore structures and super yacht design and construction.

Prof. Michael R. Davis is Professor of Engineering at the University of Tasmania. He is currently working in the area of ship dynamics and propulsion, with particular reference to high speed ship motion and wave loads, and has published and acted as consultant in heat transfer, fluid dynamics, vibration and noise. Professor Davis is a Fellow of the Institution of Engineers, Australia and a Fellow of the Royal Aeronautical Society.

Dr Giles A. Thomas is a Senior Lecturer at the Australian Maritime College, an institute of the University of Tasmania. He received his PhD in 2003 from the University of Tasmania for his work on the slamming of large high-speed catamarans. He is currently a Chief Investigator on a collaborative project with Incat and Revolution Design investigating asymmetric and non-linear loads on high-speed catamarans.

Dr Damien S. Holloway is a lecturer in Civil Engineering in the School of Engineering at the University of Tasmania. He has carried out research into ship hydrodynamics and structural mechanics and has also worked as a civil engineering consultant.